*Int. J. Heat Mass Transfer.* Vol. 28, No. 3, pp. 563–571, 1985
Printed in Great Britain

0017–9310/85 $3.00 + 0.00


# A boundary-layer analysis for natural convection in vertical porous enclosures—use of the Brinkman-extended Darcy model

T. W. TONG and E. SUBRAMANIAN
Department of Mechanical Engineering, University of Kentucky, Lexington, KY 40506, U.S.A.

(*Received* 30 *March* 1984 *and in final form* 23 *August* 1984)

**Abstract**—A boundary-layer solution for natural convection in rectangular enclosures containing a porous medium is presented. The Brinkman-extended Darcy model, which allows the no-slip boundary condition to be satisfied, is used in the formulation. The method of solution is based on the modified Oseen technique. The flow field is found to be governed by the parameter $E = Ra_0 Da/A$. Except in a thin region next to a wall, as $E \to 0$ the flow field is similar to that given by a pure Darcy analysis. Based on results obtained for the Nusselt number, it is determined that a pure Darcy analysis is applicable when $E <$ orderof $10^{-4}$. The accuracies of the present solution and the solution obtained from a pure Darcy approach are examined.

## 1. INTRODUCTION

DARCY'S law has been the momentum equation used in many studies on fluid flow in porous media [1–9]. Because Darcy's law is of order one less than the Navier–Stokes equation only the impermeable boundary condition at a surface can be satisfied, while the no-slip boundary condition cannot. In a review article Cheng [8] has noted that, for the case of natural convection in a horizontal planar porous medium bounded by a hot wall at the bottom and a cold wall at the top, Darcy's law is valid when the Darcy number ($Da$) based on the height of the porous medium is less than $10^{-3}$. A numerical study performed by Chan *et al.* [10] on natural convection heat transfer across two-dimensional enclosures containing porous materials has yielded a similar criterion for the validity of Darcy's law. Chan *et al.* used the Brinkman-extended Darcy model, which included the viscous force terms, in their analysis and were able to satisfy both the impermeable and no-slip boundary conditions. They found that when $Da$, defined in terms of the width of the enclosure, was less than $10^{-3}$ the results were independent of $Da$. Thus Chan *et al.* inferred that the inclusion of the viscous forces, and consequent satisfaction of the no-slip boundary condition, gave virtually the same result as a pure Darcy's law analysis. Chan *et al.*'s finding was, however, based largely on results for modified Rayleigh numbers ($Ra_0$) less than 300. One objective of the present work is to investigate the effect of the no-slip boundary condition and examine the validity of Darcy's law for natural convective flows with high $Ra_0$ ($\lesssim 300$). Attention will be focused on flows in two-dimensional rectangular enclosures with $Ra_0$ sufficiently high to allow exhibition of boundary-layer characteristics. We accomplish this objective by using the modified Oseen method [1, 11] to solve the boundary-layer equations, which were derived from the Brinkman's extended model [12], and comparing the results to those obtained from the Darcy model [1].

The second objective of this work is to examine the doubts that were raised by some investigators [4, 5, 7] concerning the accuracy of the boundary-layer solution presented by Weber[1]. For instance, by replacing Weber's impermeable horizontal boundary conditions with adiabatic boundary conditions, Bejan modified Weber's boundary-layer solution and was able to obtain much better agreement with experimental results [13]. Simpkins and Blythe [5], in a later work using an integral method, arrived at similar results. In these works [5, 7] comparisons were made for Nusselt numbers for low to moderately high $Ra_0$ (38–162) only. These are conditions for which the flow is at best marginally in the boundary-layer limit. Bankvall [14], based on his numerical results, suggested boundary layers might form when $Ra_0$ was approx. 150 and the experimental results of Klarsfeld [13] and Bories and Combarnous [15] did not show any boundary layers until $Ra_0 \gtrsim 300$. In the present study we will investigate the accuracy of Weber's solution by examining results that include those for $Ra_0$ higher than 162.

In Section 2, we will cover the mathematical details for obtaining a boundary-layer solution using the Brinkman-extended Darcy model. In Section 3, results showing the differences between the present solution and Weber's solution will be presented and conditions where these solutions are applicable will be established. Comparisons of results among those obtained in the present study and those from the literature [1, 5, 7, 13] will be made in Section 4.

## 2. ANALYSIS

The geometry of the problem considered is shown in Fig. 1. A two-dimensional rectangular enclosure with

## NOMENCLATURE

| | |
|---|---|
| $A$ | aspect ratio, see equation (11) |
| $A_n$ | coefficients in equation (16) |
| $d$ | width of the enclosure |
| $Da$ | Darcy number, see equation (11) |
| $DEN$ | function defined in Appendix B |
| $E$ | see definition in equation (11) |
| $f$ | functions defined in Appendix B |
| $F$ | functions defined in Appendix B |
| $g$ | gravitational acceleration |
| $L$ | height of the enclosure |
| $l$ | boundary-layer thickness, see equation (11) |
| $Nu$ | Nusselt number, see equation (31) |
| $NUM$ | function defined in Appendix B |
| $p$ | an even function defined in equation (24a) |
| $\bar{P}$ | perturbation pressure |
| $q$ | an odd function defined in equation (24b) |
| $Ra_0$ | modified Rayleigh number, see equation (11) |
| $\bar{T}$ | temperature |
| $T$ | dimensionless temperature |
| $\bar{T}_m$ | mean temperature, $(\bar{T}_h+\bar{T}_c)/2$ |
| $T_0$ | dimensionless core temperature |
| $\Delta\bar{T}$ | difference between hot and cold wall temperatures, $\bar{T}_h-\bar{T}_c$ |
| $\bar{u}$ | horizontal velocity |
| $u$ | dimensionless horizontal velocity |
| $\bar{v}$ | vertical velocity |
| $v$ | dimensionless vertical velocity |
| $\bar{x}$ | horizontal coordinate |
| $x$ | dimensionless horizontal coordinate |
| $x_{max}$ | dimensionless horizontal location when $v$ is maximum |
| $\bar{y}$ | vertical coordinate |
| $y$ | dimensionless vertical coordinate. |

Greek symbols

| | |
|---|---|
| $\alpha$ | effective thermal diffusivity |
| $\beta$ | thermal expansion coefficient |
| $\theta$ | dimensionless temperature, see equation (12) |
| $\kappa$ | permeability |
| $\lambda$ | variable in the characteristic equation (17) |
| $\lambda_n$ | roots of the characteristic equation (17) |
| $\mu$ | viscosity of the fluid |
| $\nu$ | kinematic viscosity of the fluid |
| $\rho$ | density of the fluid |
| $\phi$ | dimensionless stream function, see equation (13) |
| $\bar{\psi}$ | stream function |
| $\psi$ | dimensionless stream function |
| $\psi_0$ | dimensionless core stream function. |

Subscripts

| | |
|---|---|
| A | average |
| c | cold wall |
| h | hot wall. |

the vertical walls held at different constant temperatures is filled with a fluid-saturated porous medium. The horizontal walls are considered adiabatic. Assuming the solid and the fluid are in thermal equilibrium, we can write the governing equations from the Brinkman-extended Darcy model as [10]:

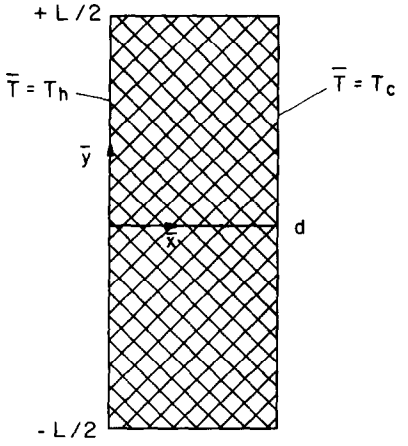


FIG. 1. Geometry of the system.

continuity

$$\frac{\partial\bar{u}}{\partial\bar{x}}+\frac{\partial\bar{v}}{\partial\bar{y}}=0, \tag{1}$$

momentum

$$\frac{\mu}{\kappa}\bar{u}=-\frac{\partial\bar{P}}{\partial\bar{x}}+\mu\left(\frac{\partial^2\bar{u}}{\partial\bar{x}^2}+\frac{\partial^2\bar{u}}{\partial\bar{y}^2}\right), \tag{2a}$$

$$\frac{\mu}{\kappa}\bar{v}=-\frac{\partial\bar{P}}{\partial\bar{y}}+\mu\left(\frac{\partial^2\bar{v}}{\partial\bar{x}^2}+\frac{\partial^2\bar{v}}{\partial\bar{y}^2}\right)+\rho g\beta(\bar{T}-\bar{T}_m), \tag{2b}$$

energy

$$\bar{u}\frac{\partial\bar{T}}{\partial\bar{x}}+\bar{v}\frac{\partial\bar{T}}{\partial\bar{y}}=\alpha\left(\frac{\partial^2\bar{T}}{\partial\bar{x}^2}+\frac{\partial^2\bar{T}}{\partial\bar{y}^2}\right), \tag{3}$$

where the symbols are as previously defined. In deriving the above equations, the Boussinesq approximation has been used for the buoyancy term and constant properties have been assumed. Note also that the viscosities associated with the term on the LHS and the second derivative terms on the RHS of equations (2a) and (2b) have been assumed equal [10].

Cross-differentiating equations (2a) and (2b) and eliminating the pressure terms, we transform equations (1) through (3) to the following:

$$-\frac{\mu}{\kappa}\left(\frac{\partial^2\bar{\psi}}{\partial\bar{x}^2}+\frac{\partial^2\bar{\psi}}{\partial\bar{y}^2}\right)=-\mu \times\left[\frac{\partial^4\bar{\psi}}{\partial\bar{x}^4}+2\frac{\partial^4\bar{\psi}}{\partial\bar{x}^2\,\partial\bar{y}^2}+\frac{\partial^4\bar{\psi}}{\partial\bar{y}^4}\right]+g\beta\frac{\partial(\bar{T}-\bar{T}_m)}{\partial x}, \quad (4)$$

$$\bar{u}\frac{\partial\bar{T}}{\partial\bar{x}}+\bar{v}\frac{\partial\bar{T}}{\partial\bar{y}}=\alpha\left(\frac{\partial^2\bar{T}}{\partial\bar{x}^2}+\frac{\partial^2\bar{T}}{\partial\bar{y}^2}\right), \quad (5)$$

where

$$\bar{u}=\frac{\partial\bar{\psi}}{\partial\bar{y}}, \quad \bar{v}=-\frac{\partial\bar{\psi}}{\partial\bar{x}}. \quad (6)$$

The boundary conditions on $\bar{\psi}$ and $\bar{T}$ are:

$$\text{at} \quad \bar{x}=0, \quad \bar{\psi}=0, \quad \frac{\partial\bar{\psi}}{\partial\bar{x}}=0, \quad \bar{T}=\bar{T}_h,$$

$$\text{at} \quad \bar{x}=d, \quad \bar{\psi}=0, \quad \frac{\partial\bar{\psi}}{\partial\bar{x}}=0, \quad \bar{T}=\bar{T}_c,$$

$$\text{at} \quad \bar{y}=\pm\frac{L}{2}, \quad \bar{\psi}=0, \quad \frac{\partial\bar{\psi}}{\partial\bar{y}}=0, \quad \frac{\partial\bar{T}}{\partial\bar{y}}=0.$$

The boundary-layer approximations to equations (4) and (5) can be obtained by performing an order of magnitude analysis [1, 11]. The thickness of the boundary layer, $l$, is taken as the horizontal length scale and is assumed to be small compared with the vertical height of the cavity $L$. Using the relation for the stream function and the velocities [equation (6)] one can find that a balance between the convection and conduction terms in equation (5) requires

$$\bar{\psi}\sim\alpha\frac{L}{l}. \quad (7)$$

A balance between the buoyancy term and the $\partial^2\bar{\psi}/\partial\bar{x}^2$ term in equation (4) requires

$$l^2\sim\frac{\nu\alpha L}{g\beta\Delta\bar{T}\kappa}. \quad (8)$$

Relations (7) and (8) are used to define the scales for the stream function and the horizontal coordinate. When the following dimensionless variables are used,

$$x=\frac{\bar{x}}{l}, \quad y=\frac{\bar{y}}{d}, \quad \psi=\frac{\bar{\psi}}{\alpha L/l},$$

$$u=\frac{\partial\psi}{\partial y}=\frac{\bar{u}d}{\alpha L/l}, \quad v=-\frac{\partial\psi}{\partial x}=\frac{\bar{v}l}{\alpha L/l},$$

$$T=(\bar{T}-\bar{T}_m)/\Delta\bar{T},$$

the approximate forms of equations (4) and (5) can be obtained as

$$\frac{\partial v}{\partial x}=E\frac{\partial^3 v}{\partial x^3}+\frac{\partial T}{\partial x}, \quad (9)$$

$$u\frac{\partial T}{\partial x}+v\frac{\partial T}{\partial y}=\frac{\partial^2 T}{\partial x^2}, \quad (10)$$

where

$$l^2=\frac{\nu\alpha L}{g\beta\Delta\bar{T}\kappa}, \quad E=\frac{Ra_0 Da}{A},$$

$$Ra_0=\frac{g\beta\Delta\bar{T}\kappa d}{\nu\alpha}, \quad Da=\frac{\kappa}{d^2}, \quad A=\frac{L}{d}. \quad (11)$$

In arriving at equation (9), the assumption that $Da\to 0$ and $Ra\to\infty$ has been invoked so that the term involving $\partial^4\psi/\partial x^2\,\partial y^2$ can be assumed negligible when compared to the first term in the equation. Defining the boundary-layer variables as [1, 11]

$$T=T_0(y)+\theta(x,y) \quad (12)$$

$$\psi=\psi_0(y)+\phi(x,y) \quad (13)$$

where $\theta$ and $\phi\to 0$ as $x\to\infty$, we can establish the necessary boundary conditions:

$$\text{at} \quad x=0, \quad \psi=0, \quad (14a)$$

$$v=0, \quad (14b)$$

$$T=\frac{1}{2}, \quad (14c)$$

$$\text{as} \quad x\to\infty, \quad \psi=\psi_0(y), \quad (15a)$$

$$T=T_0(y). \quad (15b)$$

Equations (9) and (10) are solved using the modified Oseen method. The procedure is similar to that laid out by Gill [11], who used the method to solve the boundary-layer equations for Newtonian fluid convection in an enclosure. Equation (10) is linearized by replacing $u$ and $\partial T/\partial y$ by $u_A$ and $T'_A$, which are quantities averaged across the boundary layer and are unknown odd and even functions of $y$, respectively. The prime denotes the derivative with respect to $y$. Examining equations (4) and (5) and the boundary conditions, one sees that the solutions for the temperature and flow fields are centro-symmetrical. Hence it is sufficient to analyze only one boundary layer. In this study the boundary layer along the hot wall is considered. The following outlines the important steps involved in solving the equations.

Combining equations (9) and (10) to eliminate terms $\partial T/\partial x$ and $\partial^2 T/\partial x^2$, one obtains the following differential equation

$$\frac{\partial^4 v}{\partial x^4}-u_A\frac{\partial^3 v}{\partial x^3}-\frac{1}{E}\frac{\partial^2 v}{\partial x^2}+\frac{u_A}{E}\frac{\partial v}{\partial x}+\frac{T'_A}{E}v=0.$$

The solution to this equation is of the form

$$v=\sum_{n=1}^{4}A_n(y)\,e^{-\lambda_n(y)x} \quad (16)$$

where $A_n$ are unknown coefficients and $\lambda_n$ are the roots of the characteristic equation

$$\lambda^4+u_A\lambda^3-\frac{1}{E}\lambda^2-\frac{u_A}{E}\lambda+\frac{T'_A}{E}=0. \quad (17)$$

In general, both $A_n$ and $\lambda_n$ can be functions of $y$. Since only the roots with positive real part will satisfy the

boundary condition as $x \to \infty$ and there are only two such roots (see Appendix A), one can write

$$v = A_1(y)e^{-\lambda_1(y)x} + A_2(y)e^{-\lambda_2(y)x}, \quad (18)$$

with $\lambda_1(y)$ and $\lambda_2(y)$ being the roots with positive real parts.

Equation (18) is substituted in equation (9) and a differential equation for $T$ (or for $\theta$) is obtained. Simultaneous application of the boundary conditions in equations (14b), (14c) and (15b) to the solution of this differential equation and to equation (18) yields

$$v = -\frac{1/2 - T_0}{E(\lambda_1^2 - \lambda_2^2)}(e^{-\lambda_1 x} - e^{-\lambda_2 x}) \quad (19)$$

$$T - T_0 = \theta = \frac{1/2 - T_0}{\lambda_1^2 - \lambda_2^2}(\lambda_1^2 e^{-\lambda_1 x} - \lambda_2^2 e^{-\lambda_2 x}) + v. \quad (20)$$

Once $T_0$, $\lambda_1$ and $\lambda_2$ are determined, $v$ and $T$ are completely specified by equations (19) and (20), respectively. The next step is to relate $u_A$ and $T_A$ to the core values $u_0$ and $T_0$. Integration of the expression $v = -\partial\psi/\partial x$ with respect to $x$ and the use of equations (14a) and (15a) leads to

$$\psi_0 = -\frac{1/2 - T_0}{E\lambda_1\lambda_2(\lambda_1 + \lambda_2)}. \quad (21)$$

Similarly integration of equation (10) and combination with equations (19) and (20) yields

$$\frac{d}{dy}\frac{(1/2 - T_0)^2(E\lambda_1\lambda_2 + 1)}{2E^2(\lambda_1 + \lambda_2)^3\lambda_1\lambda_2} - \psi_0 T_0' = \frac{1/2 - T_0}{E(\lambda_1 + \lambda_2)} \times [E(\lambda_1 + \lambda_2)^2 - E\lambda_1\lambda_2 - 1]. \quad (22)$$

As discussed by Gill [11], the following relations are true for $\lambda_1$, $\lambda_2$, $\lambda_3$ and $\lambda_4$

$$\lambda_3(y) = -\lambda_1(-y) \quad (23a)$$

$$\lambda_4(y) = -\lambda_2(-y). \quad (23b)$$

Thus introducing an even function $p$ and an odd function $q$ as

$$p(y) = \lambda_1 + \lambda_2 - \lambda_3 - \lambda_4 \quad (24a)$$

$$q(y) = \frac{u_A}{p} \quad (24b)$$

and combining with equations (A2) through (A4), we obtain

$$\lambda_1 + \lambda_2 = p(1 - q)/2 \quad (25a)$$

$$\lambda_1\lambda_2 = p^2(1 - q^2)(1 - q)/8 - (1 + q)/2E \quad (25b)$$

$$\lambda_1, \lambda_2 = \frac{1}{4E}[Ep(1 - q) \pm i\sqrt{Ep^2(1 - q^2)(1 + 2q) - 8E(1 + q)}]. \quad (25c)$$

Equations (25a) and (25b) are substituted in equation (21) to yield

$$\psi_0 = -\frac{16(1/2 - T_0)}{[Ep^2(1 - q^2) - 4]p(1 - q^2)}. \quad (26)$$

By transforming $y \to -y$ and observing that $q$ and $T_0$ are odd, and $p$ and $\psi_0$ are even functions of $y$, we obtain

$$T_0 = \frac{gp^2E}{Ep^2 + Ep^2q^2 - 4} \quad (27a)$$

$$\psi_0 = -\frac{8}{p(1 - q^2)(p^2E + p^2q^2E - 4)}. \quad (27b)$$

Substitution of equations (25a), (25b), (27a) and (27b) into equation (22) results in an equation involving $p$, $q$, $p'$ and $q'$. By transforming $y \to -y$ and taking into account the odd and even nature of the functions, one can obtain another equation involving the same set of functions ($p$, $q$, $p'$ and $q'$). These two equations are rearranged to give $p$ and $q$ in terms of a pair of coupled ordinary differential equations. They are

$$p' = \frac{f_4(p, q)F_2(p, -q) - f_4(p, -q)F_2(p, q)}{F_1(p, q)F_2(p, -q) + F_1(p, -q)F_2(p, q)} \quad (28a)$$

and

$$q' = \frac{f_4(p, -q)F_1(p, q) + f_4(p, q)F_1(p, q)}{F_2(p, -q)F_1(p, q) + F_2(p, q)F_1(p, -q)} \quad (28b)$$

where the $f$ and $F$ functions have been defined in Appendix B. Equations (28a) and (28b) are solved numerically subject to the following boundary conditions:

$$\text{at} \quad y = 0, \quad q = 0 \quad (29a)$$

$$\text{at} \quad y = \frac{1}{2}, \quad q = -1 - \frac{2}{\sqrt{Ep}}. \quad (29b)$$

The condition in equation (29a) is obtained from equation (27a) by using the fact that $q$ is an odd function of $y$ and $T_0 = 0$ at $y = 0$. Equation (29b) corresponds to the condition that $T_0 = 1/2$ at $y = 1/2$ which is the mathematical representation of the physical assumption that all the fluid is warmed to a temperature $T = T_h = 1/2$ as it reaches the top of the hot wall [1, 11]. Once $p$ and $q$ are known, they are used in conjunction with equations (25c) and (27a) to determine $v$ and $T$ from equations (19) and (20), respectively.

Equations (28a) and (28b) were solved iteratively. By using equation (29a) and guessing the values of $p$ at $y = 0$, we marched in the $y$-direction and obtained the values of $p$ and $q$ at $y + \Delta y$. The marching process was continued until $y = 1/2$. The values of $p$ and $q$ at $y = 1/2$ were checked to see if they satisfied equation (29b). A new value of $p$ at $y = 0$ was guessed and the calculation was repeated until the condition specified by equation (29b) was met.

## 3. RESULTS AND DISCUSSION

Figure 2 shows the vertical velocity profile at mid-height of the enclosure for various values of $E$. Since

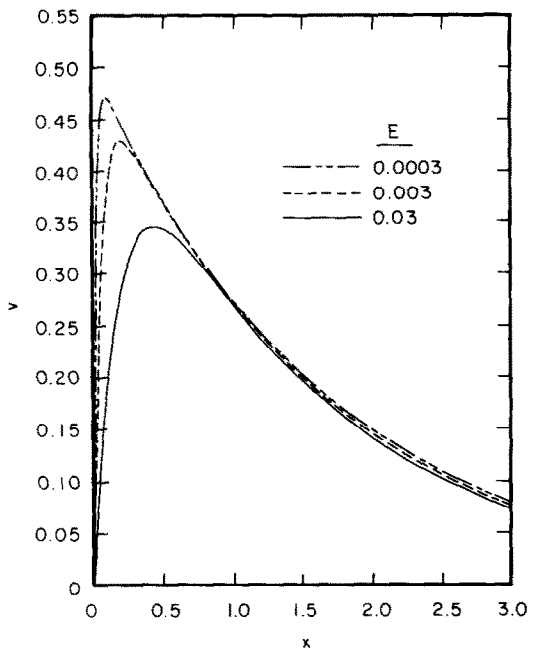


FIG. 2. The vertical velocity profile at mid-height of the enclosure.

viscous forces are accounted for in the Brinkman-extended Darcy model, the no-slip boundary condition can be satisfied and the velocity at the wall is zero. The velocity increases to a maximum and then drops back to zero as we approach the core [see equation (13)]. When $E$ decreases the peak velocity shifts toward the boundary. This trend is consistent with the model used in that the cubic term (due to Brinkman's extension) in equation (9) becomes less important as $E$ decreases. When the cubic term is neglected equation (9) reduces to the pure Darcy model [1]. Because of slip the peak velocity given by the Darcy model is exactly at the boundary. The location of the peak velocity in the present results can be obtained by solving for $x$ in equation (19) when the velocity gradient is zero. The result is

$$x_{\max} = \frac{\ln(\lambda_1/\lambda_2)}{\lambda_1 - \lambda_2}, \tag{30}$$

and the dependence of $x_{\max}$ on $E$ is shown in Fig. 3. As $E \to 0$, $x_{\max} \to 0$ asymptotically; and except in a thin region next to the wall the flow field resembles that given by a pure Darcy analysis.

The Nusselt number representing the amount of heat transfer across the enclosure can be defined as

$$Nu = \frac{\text{total heat transfer}}{\text{heat transfer by conduction only}}.$$

In terms of the variables already defined, it is

$$Nu = \left(\frac{Ra_0}{A}\right)^{1/2} \int_{-1/2}^{1/2} -\left.\frac{\partial\theta}{\partial x}\right|_{x=0} \mathrm{d}y. \tag{31}$$

Using the modified Oseen method to solve the Darcy boundary-layer equations, Weber [1] obtained the value $\sqrt{3}/3$ for the integral in equation (31). Therefore the result obtained from the Darcy model is independent of $E$. The value of the integral in the present analysis is a function of $E$ and is shown in Fig. 4. When $E \to 0$ the value from the Brinkman-extended model approaches that from the Darcy model. When $E = 1 \times 10^{-3}$ the difference between the values of the integral (and consequently the values of the Nusselt number) from the two models is 4% and when $E < 1 \times 10^{-4}$ the difference is less than 1%. Figure 5 shows the effect of $Ra_0$ and $Da$ on $Nu$ for $A = 10$. It is seen that for a given value of $Da$ the deviation from the Darcy result increases as $Ra_0$ becomes larger. This is because, when $Da$ and $A$ are held constant, $Ra_0$ is directly proportional to $E$ and as can be seen from Fig. 4 the difference between the values of the integrals from the two models increases as $E$ increases.

As mentioned in the Introduction, the criterion that has been used to establish the validity of Darcy's law is when $Da$ is smaller than a certain value [8, 10]. As is shown in this analysis, the proper parameter for

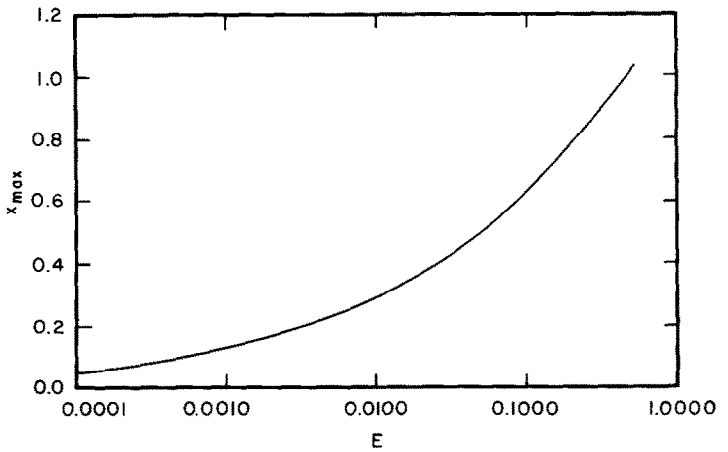


FIG. 3. Location of the peak velocity at mid-height of the enclosure.

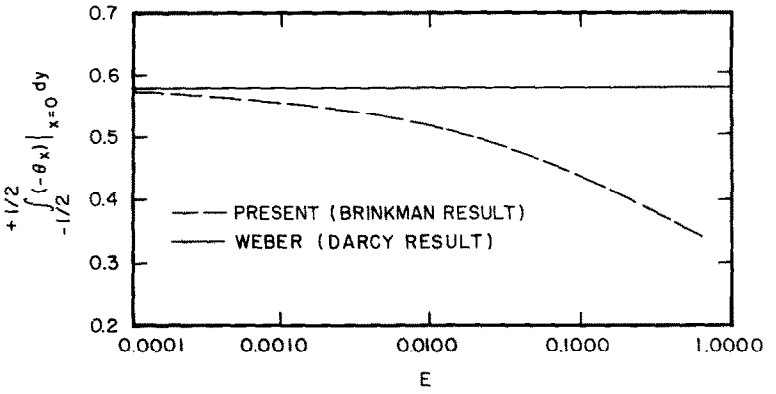


FIG. 4. Comparison of the Brinkman and Darcy results on the integral in equation (31).

establishing such a criterion for the present problem is $E$ rather than $Da$. Smaller $Da$ will result in smaller $E$ only if $Ra_0$ and $A$ are held constant or if the latter variables are also changed appropriately [see equation (11)]. As a guide, one may use $E <$ order of $10^{-4}$ as the criterion for the validity of Darcy's law.

## 4. COMPARISON OF RESULTS

As mentioned earlier, questions have arisen concerning the accuracy of Weber's Darcy boundary-layer solution. Since we have basically used the same method of solution, one might also question the accuracy of the present solution. Shown in Table 1 is a comparison of Nusselt numbers reported by various investigators. Klarsfeld's results [13] are actual experimental data. They will be used as bench-mark values for comparison owing to two reasons: (1) other investigators [5, 7] have compared their results with his and (2) Klarsfeld has reported all the experimental information necessary for us to determine the dimensionless variables involved in the present study.

Because $E$ is less than the order of $10^{-4}$ for most of the cases shown, the present results are the same as those obtained by Weber. For Cases 2 and 5, the present solution offers some improvement over Weber's solution when compared to the experimental data. The improvement is more noticeable for larger $Ra_0$.

The asterisked values are those that have been used in comparisons conducted by other investigators [5, 7]. As claimed by Bejan [7], his results agree with those experimental data asterisked under Cases 1, 3 and 4 better than do Weber's. If we consider Case 5 where we have a higher $A$ and moderate to high $Ra_0$, Weber's solution is seen to be just as accurate as Bejan's. The present solution, which is a higher order approximation than Weber's, since viscous forces have been included in the formulation, offers the best agreement with the experimental results.

From the above comparison, it is apparent that Weber's solution is accurate and useful for predicting $Nu$ when (1) $E$ is small, (2) $Ra_0 \lesssim 150$ and (3) $A = 4.5$. Although not supported by the results shown in Table 1, we believe the latter restriction can be stated more

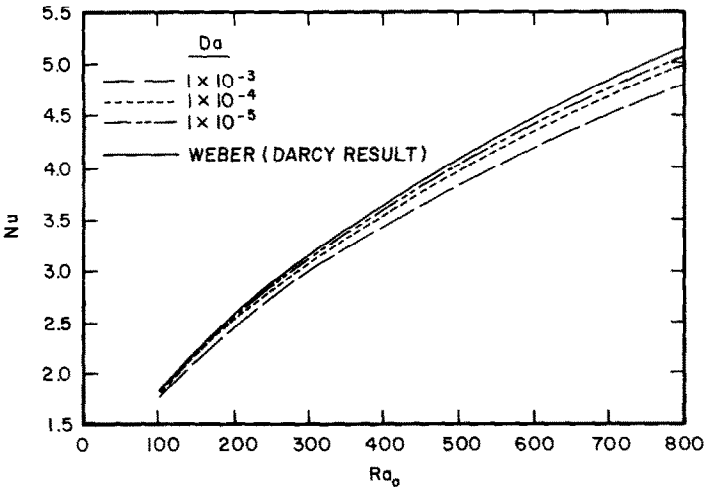


FIG. 5. Comparison of the Brinkman and Darcy results on the Nusselt number for $A = 10$.

Table 1. Comparison of results on the Nusselt number

| Case | $A$ | $Da$ | $Ra_0$ | $E = Ra_0 Da/A$ | Klarsfeld [13] | Weber [1] | Bejan [7] | Walker and Homsy [4] | Simpkins and Blythe [5] | Present |
|---|---|---|---|---|---|---|---|---|---|---|
| 1 | 2.25 | $1.188 \times 10^{-7}$ | 47.9 | $2.53 \times 10^{-6}$ | 2.2* | 2.7 | 2.2 | 2.4 | 2.4 | † |
| | | | 91.6 | $4.84 \times 10^{-6}$ | 3.0* | 3.7 | 3.1 | 3.3 | 3.3 | † |
| | | | 147.6 | $7.79 \times 10^{-6}$ | 3.8* | 4.7 | 4.0 | 4.1 | 4.2 | † |
| | | | 200.6 | $1.06 \times 10^{-5}$ | 4.5 | 5.5 | 4.8 | 4.8 | 4.9 | † |
| | | | 252.4 | $1.33 \times 10^{-5}$ | 5.2 | 6.1 | 5.4 | 5.4 | 5.5 | † |
| | | | 280.0 | $1.48 \times 10^{-5}$ | 6.0 | 6.4 | 5.7 | 5.7 | 5.8 | † |
| 2 | 2.25 | $8.125 \times 10^{-7}$ | 324.5 | $1.17 \times 10^{-4}$ | 5.7 | 6.9 | 6.2 | 6.1 | 6.2 | † |
| | | | 649.0 | $2.34 \times 10^{-4}$ | 8.3 | 9.8 | 8.9 | 8.7 | 8.8 | 9.6 |
| | | | 1298.0 | $4.69 \times 10^{-4}$ | 11.8 | 13.9 | 12.7 | 12.3 | 12.5 | 13.5 |
| | | | 1622.5 | $5.86 \times 10^{-4}$ | 13.3 | 15.5 | 14.4 | 13.7 | 13.9 | 15.0 |
| 3 | 4.50 | $1.125 \times 10^{-7}$ | 44.2 | $1.11 \times 10^{-6}$ | 1.5* | 1.8 | 1.6 | 1.6 | 1.6 | † |
| 4 | 4.50 | $3.675 \times 10^{-7}$ | 37.9 | $3.10 \times 10^{-6}$ | 1.4* | 1.7 | 1.5 | 1.5 | 1.5 | † |
| 5 | 4.50 | $3.250 \times 10^{-6}$ | 162.0 | $1.16 \times 10^{-4}$ | 3.3* | 3.5 | 3.2 | 3.1 | 3.1 | 3.4 |
| | | | 324.0 | $2.34 \times 10^{-4}$ | 4.7 | 4.9 | 4.6 | 4.3 | 4.4 | 4.8 |
| | | | 648.0 | $4.68 \times 10^{-4}$ | 6.8 | 6.9 | 6.6 | 6.1 | 6.2 | 6.8 |

* Values chosen for comparison in refs. [5] and [7].
† Same as Weber's result.

generally as $A \gtrsim 4.5$. When $E$ is not small (e.g. $E >$ order of $10^{-4}$), one should use the present boundary-layer solution with similar restrictions on $A$ and $Ra_0$.

## 5. CONCLUSION

The effect of the no-slip boundary condition for flow in porous media contained in two-dimensional rectangular enclosures has been studied. By employing the Brinkman-extended Darcy model we were able to satisfy both the no-slip and the impermeable boundary conditions. Consideration was given to flows which exhibit boundary-layer characteristics. The boundary-layer equations derived from the Brinkman-extended Darcy model were solved using the modified Oseen method [1, 11]. The flow field was found to be characterized by a parameter $E$ defined as $Ra_0 Da/A$. As $E \to 0$, the flow field resembled that given by a pure Darcy analysis except in a thin region next to a boundary. In this region, the present solution's satisfaction of the no-slip boundary condition yields a velocity profile which more closely approximates the physical situation. The Nusselt number was determined to be a function of $E$ as well as $Ra_0$ and $A$. We propose that $E <$ order of $10^{-4}$ be used as the criterion for the validity of Darcy's law for the present problem. When the above restriction on $E$ was met, we found that the Darcy results agreed with the present results to within 1%. A comparison with Klarsfeld's experimental data [13] demonstrated that Weber's Darcy boundary-layer solution [1] and the present boundary-layer solution were accurate when $Ra_0 \gtrsim 150$ and $A \gtrsim 4.5$.

*Acknowledgement*—The authors are grateful for the support of this work by the National Science Foundation through grant DME-8105951.

## REFERENCES

1. J. E. Weber, The boundary-layer regime for convection in a vertical porous layer, *Int. J. Heat Mass Transfer* **18**, 569–573 (1975).
2. R. J. Ribando and K. E. Torrance, Natural convection in a porous medium: effects of confinement, variable permeability, and thermal boundary conditions, *J. Heat Transfer* **98**, 42–48 (1976).
3. P. J. Burns, L. C. Chow and C. L. Tien, Convection in a vertical slot filled with porous insulation, *Int. J. Heat Mass Transfer* **20**, 919–926 (1977).
4. K. L. Walker and G. M. Homsy, Convection in a porous cavity, *J. Fluid Mech.* **87**, 449–474 (1978).
5. P. G. Simpkins and P. A. Blythe, Convection in a porous layer, *Int. J. Heat Mass Transfer* **23**, 881–887 (1980).
6. C. E. Hickox and D. K. Gartling, A numerical study of natural convection in a horizontal porous layer subjected to an end-to-end temperature difference, *J. Heat Transfer* **103**, 797–802 (1981).
7. A. Bejan, On the boundary layer regime in a vertical enclosure filled with a porous medium, *Letters Heat Mass Transfer* **6**, 93–102 (1979).
8. P. Cheng, Heat transfer in geothermal systems, *Adv. Heat Transfer* **14**, 1–105 (1978).
9. T. W. Tong, R. C. Birkebak and I. E. Enoch, Thermal radiation, convection, and conduction in porous media contained in vertical enclosures, *J. Heat Transfer* **105**, 414–418 (1983).
10. B. K. C. Chan, C. M. Ivey and J. M. Barry, Natural convection in enclosed porous media with rectangular boundaries, *J. Heat Transfer* **92**, 21–27 (1970).
11. A. E. Gill, The boundary-layer regime for convection in a rectangular cavity, *J. Fluid Mech.* **26**, 515–536 (1966).
12. H. C. Brinkman, A calculation of the viscous force exerted by a flowing fluid on a dense swarm of particles, *Appl. Sci. Res.* **A1**, 27–34 (1947).
13. S. Klarsfeld, Champs de temperature associes aux mouvements de convection naturelle dans un milieu poreux limite, *Rev. Gen. Thermique* **9**, 1403–1423 (1963).
14. C. G. Bankvall, Natural convective heat transfer in insulated structures, Lund Inst. of Tech. Report 38 (1972).
15. S. A. Bories and M. A. Combarnous, Natural convection in a sloping porous layer, *J. Fluid Mech.* **57**, 63–79 (1973).

## APPENDIX A

For $\lambda_n$ to be the roots of equation (17), it is required that

$$(\lambda-\lambda_1)(\lambda-\lambda_2)(\lambda-\lambda_3)(\lambda-\lambda_4)=0. \tag{A1}$$

Comparing equations (17) and (A1) we obtain

$$u_A=-\lambda_1-\lambda_2-\lambda_3-\lambda_4, \tag{A2}$$

$$-\frac{1}{E}=\lambda_1\lambda_2+\lambda_1\lambda_3+\lambda_1\lambda_4+\lambda_2\lambda_3+\lambda_2\lambda_4+\lambda_3\lambda_4, \tag{A3}$$

$$\frac{u_A}{E}=\lambda_1\lambda_2\lambda_3+\lambda_1\lambda_2\lambda_4+\lambda_1\lambda_3\lambda_4+\lambda_2\lambda_3\lambda_4, \tag{A4}$$

$$\frac{T'_A}{E}=\lambda_1\lambda_2\lambda_3\lambda_4. \tag{A5}$$

Since the fluid is warmed as it flows upward along the hot wall, $T'_A>0$. Therefore equation (A5) admits the following possibilites: (a) all of the real parts of $\lambda_n$ are of the same sign, (b) two $\lambda_n$ have positive real parts while the other two have negative real parts. To satisfy equation (A3), however, only possibility (b) above can be true.

## APPENDIX B

$$F_1=\frac{f_{11}}{DEN}-\frac{NUM}{DEN^2}f_{21}-\frac{f_{31}}{f_{34}f_{33}^2}$$

$$F_2=\frac{f_{12}}{DEN}-\frac{NUM}{DEN^2}f_{22}-\frac{f_{32}}{f_{34}f_{33}^2}$$

$$NUM=[Ep^2(1+q^2-2q)-4][Ep^2-Ep^2q^2-4]$$

$$DEN=Ep^3(Ep^2+Ep^2q^2-4)^2(1-q)(1-q^2)$$

$$f_4=f_{41}f_{42}$$

$$f_{11}=-4E^2p^3q^4+8E^2p^3q^3+16Epq^2-8E^2p^3q-16Epq+4E^2p^3$$

$$f_{12}=-4E^2p^4q^3+6E^2p^4q^2+16Ep^2q-2E^2p^4-8Ep^2$$

$$f_{21}=7E^3p^6q^2(1-q^2+q^3)+40E^2p^4(-1+q+q^4-q^5)+7E^3p^6(1-q-q^6+q^7)+48Ep^2(1-q^2-q+q^3)$$

$$f_{22}=E^3p^7q(2-4q^2-3q+5q^3)+8E^2p^5q^3(1-5q)E^3p^7(-1-6q^5+7q^6)+16Ep^3(1-2q+3q^2)$$

$$f_{31}=-8Epq$$

$$f_{32}=E^2p^4-4Ep^2-E^2p^4q^2$$

$$f_{33}=Ep^2+E^2p^2q^2-4$$

$$f_{34}=-p(1-q^2)(Ep^2+Ep^2q^2-4)/8$$

$$f_{41}=\frac{Ep^2+E^2p^2-2Ep^2q^2-4}{8Ep(1-q)(Ep^2+Ep^2q^2-4)}$$

$$f_{42}=2Ep^2(1-q^2)-Ep^2(1-q^2)(1-q)+4q-4.$$


## UNE ANALYSE DE COUCHE LIMITE POUR LA CONVECTION NATURELLE DANS LES CAVITES POREUSES VERTICALES, A PARTIR DU MODELE DE DARCY ETENDU SELON BRINKMAN

**Résumé**—On présente une solution de couche limite pour la convection naturelle dans des cavités rectangulaires contenant un milieu poreux. Le modèle élargi Darcy–Brinkman qui satisfait la condition à la limite de non-glissement, est utilisé dans la formulation. La méthode de résolution est basée sur la technique d'Oseen avec modification. Le champ d'écoulement est gouverné par le paramètre $E = Ra\,Da/A$. Excepté dans une mince région proche de la paroi, lorsque $E \to 0$ l'écoulement est semblable à celui donné par une simple analyse de Darcy. A partir des résultats sur le nombre de Nusselt, on vérifie qu'une analyse de Darcy est applicable quand $E$ est inférieur à $10^{-4}$. On examine aussi les précisions de la solution donnée et de la solution obtenue par l'approche simple selon Darcy.



## UNTERSUCHUNG DER GRENZSCHICHT BEI NATÜRLICHER KONVEKTION IN EINEM SENKRECHTEN HOHLRAUM, DER MIT EINEM PORÖSEN MEDIUM GEFÜLLT IST VERWENDUNG DES NACH BRINKMAN ERWEITERTEN DARCY-MODELLS

**Zusammenfassung**—Die Lösung der Grenzschichtgleichung bei natürlicher Konvektion in einem rechteckigen Hohlraum, der ein poröses Medium enthält, wird dargestellt. Das nach Brinkman erweiterte Darcy-Modell, das die Haftbedingung an der Wand erfüllt, wird beim Ansatz verwendet. Die Lösung basiert auf der modifizierten Methode von Oseen. Das Strömungsfeld wird durch den Parameter $E = Ra_0\,Da/A$ bestimmt. Lediglich in einer dünnen Schicht in Wandnähe, wenn $E \to 0$, ist das Strömungsfeld ähnlich dem, das man mit dem reinen Darcy-Modell erhält. Aufgrund der Nusselt-Zahl wird festgestellt, daß das reine Darcy-Modell für $E <$ etwa $10^{-4}$ anwendbar ist. Die Genauigkeiten der vorliegenden Lösung und der Lösung, die man mit dem reinen Darcy-Modell erhält, werden untersucht.

## РЕШЕНИЕ ЗАДАЧИ ПОГРАНИЧНОГО СЛОЯ ДЛЯ ЕСТЕСТВЕННОЙ КОНВЕКЦИИ В ВЕРТИКАЛЬНЫХ ПОРИСТЫХ ПОЛОСТЯХ—ИСПОЛЬЗОВАНИЕ МОДЕЛИ БРИНКМАНА-ДАРСИ

**Аннотация**—Представлено решение задачи пограничного слоя для естественной конвекции в прямоугольных полостях, заполненных пористой средой. В постановке задачи используется модель Бринкмана-Дарси, которая позволяет удовлетворить условию прилипания на границе. Способ решения основывается на модифицированной методике Озеена. Обнаружено, что поле скоростей определяется параметром $E = Ra_0\, Da/A$. За исключением небольшой прилегающей к стенке области, где $E \to 0$, поле скоростей подобно полученному в приближении Дарси. На основании результатов, полученных для числа Нуссельта, найдено, что чистый анализ Дарси применим при $E < \sim 10^{-4}$. Исследуются точности представленного решения и решения, полученного из приближения Дарси.